A&A 429, 247–255 (2005)
DOI: 10.1051/0004-6361:20041446
© ESO 2004

Astronomy & Astrophysics

New insights in the FUV into the activity of the Herbig Ae star HD 163296

M. Deleuil[1], J.-C. Bouret[1], C. Catala[2], A. Lecavelier des Etangs[3], A. Vidal-Madjar[3], A. Roberge[4], P. D. Feldman[5], C. Martin[1], and R. Ferlet[3]

[1] Laboratoire d'Astrophysique de Marseille, CNRS - Université de Provence, BP 8, 13376 Marseille Cedex 12, France
e-mail: magali.deleuil@oamp.fr
[2] Observatoire de Paris-Meudon, CNRS, Paris, France
[3] Institut d'Astrophysique de Paris, 98bis Bd Arago, 75014 Paris, France
[4] Dept. of Terrestrial Magnetism, Carnegie Institution of Washington, 5241 Broad Branch Rd., Washington, DC 20015-1305, USA
[5] Dept. of Physics and Astronomy, Johns Hopkins University, 3400 N. Charles St., Baltimore, Maryland 21218, USA

Received 10 June 2004 / Accepted 28 July 2004

Abstract. We present an analysis of the *FUSE* spectra of HD 163296, a young isolated Herbig Ae star. The spectra in the far UV spectral range are dominated by strong emission lines of C III and O VI, which exhibit broad and complex asymmetric profiles with wings extending over more than 1000 km s^{-1}. The H I Ly α and the C III emission profiles show evidence for an outflow with a terminal velocity of 270 km s^{-1}. We also identified several narrower emission lines due to fluorescent decays in Fe II. Using an HST/STIS archive spectrum, we checked that the H I Ly α line, which has a clear type III P Cygni emission profile, is broad enough to provide the photons required to photo-excite the Fe II upper levels. As previously explored for the well-known Herbig Ae star AB Aur, most of the spectral features including the fluorescent lines are consistent with the presence of a chromosphere above the photosphere. However, the over-ionized species cannot be produced in this region alone and we discuss two alternative mechanisms to explain such spectral signatures: magnetospheric accretion and a magnetically confined wind. Both interpretations involve a large-scale magnetic field whose detection is now a challenge for the new generation of spectropolarimeters such as ESPaDOnS.

Key words. stars: activity – stars: individual: HD 163296 – line: profiles – line: identification – stars: magnetic fields

1. Introduction

Among pre-main sequence stars, Herbig Ae/Be stars (HAeBe) appear as a prolongation of the T Tauri star group toward higher effective temperatures and masses. Like the Classical T Tauri stars (CTTS), they exhibit infrared excess as well as irregular variability in their spectroscopic and photopolarization characteristics. Both groups appear as evolutionary precursors of the Vega-like stars such as β Pictoris (Vidal-Madjar et al. 1998), and the study of the their circumstellar (CS) environment is of critical interest as the putative site of ongoing planet formation which should take place as the stars evolve to the main sequence.

HD 163296 belongs to the small number of the so-called isolated Herbig Ae/Be stars which present the usual characteristics of the classical HAeBes, but are not embedded in a nebulosity. First classified as a young Herbig Ae/Be star by Finkenzeller & Mundt (1984), the star (A1Ve, age = 4^{+4}_{-2} Myr, d = 122 pc; van den Ancker et al. 1998) is sometimes considered as prototypical of the Herbig Ae class.

Imaging techniques provide evidence for the distribution of the circumstellar material within a disk: a disk spatially resolved, with dimension $\simeq$310 × 160 AU, was first revealed by CO mm interferometry (Mannings & Sargent 1997) and more recently, coronagraphic observations mapped an extended disk-like structure in the visible (Grady et al. 2000). Both studies agree with an inclination of the system about 60°. In addition, a subsequent study in the ultraviolet detected the presence of a bipolar outflow associated with the star (Devine et al. 2000). According to *Infrared Space Observatory* (ISO) observations, the CS dust presents a bi-modal mass over temperature distribution with a population of large grains ($\simeq$1 mm) (Bouwman et al. 2000). The composition of these grains appears to be dominated by amorphous silicates, iron oxide and water ice (Sitko et al. 1999; Bouwman et al. 2000; van den Ancker et al. 2000).

Warm CS H_2 gas ($T \simeq 430K$) has also been observed toward HD 163296 (Lecavelier des Etangs et al. 2003). Although this detection is consistent with a location of the gas within a few AU of the star at most, the exact spatial distribution of this

Article published by EDP Sciences and available at http://www.aanda.org or http://dx.doi.org/10.1051/0004-6361:20041446

medium remains to be better constrained. More interestingly, as a member of the Herbig group, the spectrum of the star from the ultraviolet (UV) to the infrared (IR), shows a rich, mostly variable, emission-line spectrum. In the visible, the Balmer lines exhibit strong variations in intensity and position with an evolution of the line shape from a double-peak to a type III P Cygni profile on time scales from one hour to several days (Thé et al. 1985; Pogodin 1994). If the Balmer lines are the most intense emission lines, many other low-ionization lines are present in the UV and in the visible and most of them exhibit similar rapid line profile variability. However, only in a few cases has periodic behaviour been seen in the analysis of temporal series of optical spectra: Catala et al. (1989) found a periodic modulation in the variations of the Mg II and Ca II resonance lines, with however, different period values: 50 ± 8 h for Mg II and 35 ± 5 h for Ca II. More recently, Beskrovnaya et al. (1998) reported the presence of likely cyclic positional variations for the Hα and Hβ emission lines as well as sinusoidal variations of the linear polarization parameters. However, depending the epoch of observations, this periodic behaviour can be masked by additional active flare-like phenomena that may dominate the variation of the line profile. Together with insufficient temporal coverage, this may explain the apparent lack of periodicity in time series analysis reported by other authors (Baade & Stahl 1989).

The observation of the star in the far ultraviolet (FUV) spectral range presented in this paper allows us to probe regions of higher temperature and complete the picture of the physical conditions of the close CS environment of HD 163296. We will discuss its characteristics and their implications in the context of two models, both involving a stellar magnetic field.

2. Observations and data reduction

HD 163296 was observed with *FUSE* on 2001 April 27 and 29, for 15 920 s and 16 197 s respectively. The observations were made in the time-tagged mode, using the $30'' \times 30''$ low-resolution aperture (LWRS). Each exposure was divided into 5 sub-exposures with exposure times between 2582 and 3558 s. These individual sub-exposures were processed with version 2.4.0 of the *CALFUSE* pipeline processing software (see Moos et al. 2000; Sahnow et al. 2000). The sub-exposures were then cross-correlated segment by segment prior to their co-addition to avoid the potential loss of co-alignment between the spectroscopic channels from one exposure to another and we did not co-add spectra from different channels. The final spectra were then re-sampled into larger bins: 8 initial pixels for the LiF segments and 7 pixels for the SiC one, as the *FUSE* spectra are highly oversampled.

To complement our FUV emission line analysis, we also used a HST/STIS high resolution observation of HD 163296 obtained from the archives. The STIS spectrum was recorded on 2000 July 22, 9 months before our *FUSE* observations. These observations cover two spectral ranges: one around H I Ly α, from 1191 to 1245 Å, which includes the Si III and the N V doublet resonance lines; the second one around the C III* UV4 multiplet, from 1145 to 1199 Å.

We took advantage of the overlap between the *FUSE* and STIS spectral domains around the C III* multiplet to establish the absolute wavelength scale by cross-correlation techniques. We found that the *FUSE* LiF2a segments are shifted by -30 ± 30 km s^{-1}. Note that according to the *SIMBAD* data base, the radial velocity of the star is –4 km s^{-1}. The offsets of the absolute wavelength calibration for the other segments were established using the H_2 absorption lines which are observed in all segments.

3. The FUV spectra

As expected for such a cool star, the photospheric spectrum of HD 163296 in the FUV spectral range is very faint, even in the long wavelength part of the *FUSE* domain. On the other hand, this low level continuum makes emission features easy to detect. The most prominent emission features are the resonance lines of C III λ977, the O VI doublet (1032, 1037 Å), and the C III* multiplet at 1776 Å (UV4) (Fig. 1). The spectra also contain several narrower emission features observed mainly between 1110 Å and 1150 Å. We identified these lines as fluorescent decays of Fe II excited levels pumped by H I Ly α (see Sect 3.2).

3.1. Hot emission line analysis

All emission lines are wide with profile wings extending to at least ± 550 km s^{-1}. Except for the C III resonance line, we noticed a clear absence of absorption features other than the superimposed narrow H_2 circumstellar absorption lines. All the lines display a blue-red asymmetry about the line center in the stellar rest frame. This asymmetry is not obvious from a simple examination of the radial velocities of the line wings, but it is highlighted by reflecting each line profile with respect to the star's rest frame velocity, as illustrated in Fig. 1.

The O VI doublet shows the most regular profile although it cannot be fit by a single Gaussian. In this case, the lines appear with a flat-topped profile which is however compatible with an unresolved double-peak.

The N V emission line profiles in the STIS spectrum appear surprisingly different from those of the O VI doublet. The observed lines indeed seem compatible with an inverse P Cygni profile: a single broad emission peak with the centroid of the 1238.8 Å emission blueshifted by 110 km s^{-1} relative to the star's rest frame, and a strong absorption feature in the red wing of the line. However, both lines of the N V doublet are strongly blended: by the Mg II resonance line at 1240.4 Å, and by the lines of the N I multiplet UV 5 at 1243.1 Å. In the case of the well-known Herbig Ae star, AB Aur, which exhibits a similar line profile in the N V doublet, Bouret et al. (1997), using a detailed model of line formation, concluded that the origin of the Mg II and N I lines was purely photospheric. The similarities between AB Aur and HD 163296 together with the width of the absorption features, allow us to draw the same conclusion. The actual N V profile could thus be similar to that of O VI but a precise estimation of the N V line profile in HD 163296 would require detailed modeling of the physical regions where the different lines are formed, which is beyond the scope of the present paper.

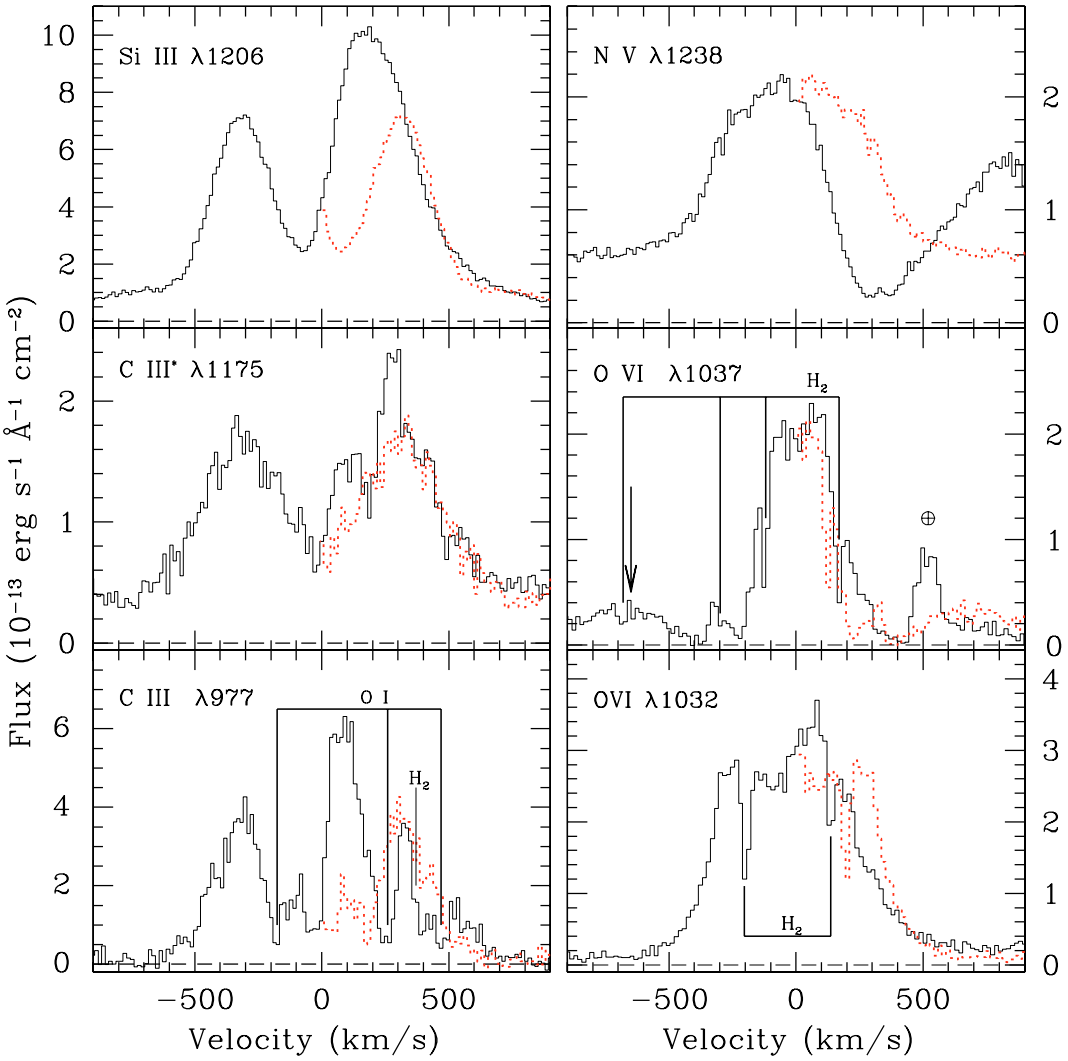

Fig. 1. FUV emission lines observed in the HD 163296 *FUSE* (2002/29/04) and HST/STIS spectra. The arrow points to the C II resonance line at 1036 Å, whereas the line labeled with the ⊕ symbol, close to the λ1037 O VI line, is an airglow emission line. The narrow H_2 absorption lines and the O I fine structure lines, superimposed on the emission profiles are indicated with tic marks. The dotted lines correspond to the blue wing of each emission line reflected about the zero velocity in the stellar rest frame and overplotted on the red wing to highlight the asymmetry of the profile. Note that the emission peak of the second component of the N V doublet at 1242 Å is apparent at about +850 km s^{-1} from the first component.

The C III resonance line profile is very different from that of the C III* multiplet, which displays a clear double-peaked profile. The resonance line presents a strong, slightly redshifted emission peak with an extended red wing and a blueshifted emission peak of moderate intensity. It is surprisingly similar to the one we previously observed in the *FUSE* spectrum of the Herbig Be star, HD 100546 (Deleuil et al. 2004). Absorption features are superimposed on the profile: the narrowest ones are due to H_2 electronic transitions and the broadest to O I resonance fine-structure transitions. A broad absorption feature appears in both exposures at a velocity of –58 km s^{-1} which can be related to an outflow in C III.

Two weak and broad emission features are also marginally detected: one in the blue wing of the O VI λ1037 line, indicated by an arrow in Fig. 1, and a second one observed at 933.2 Å. Following the analysis of the *FUSE* spectrum of HD 100546 (Deleuil et al. 2004), the first emission feature is identified as the blue wing of an emission line due to the C II resonance line at 1036 Å. The line at 933.2 Å could be due to a resonance transition of S VI, but with a single observed line this identification still needs to be confirmed.

Finally, we also identified a few weak emission features at 1017.8 Å, 1021.6 Å, 1064.1 Å and 1072.1 Å for which we could not find any reliable identification.

Turning to the other emission lines observed with HST, we found that the Si III emission line displays a double-peaked profile, very similar to that of C III* (Fig. 1). The time-lag between the two spectra does not allow a direct comparison of the two line profiles. However, if in the C III* line the blue and red emission peaks have nearly the same intensity, the red peak in Si III line is clearly more intense than the blue one. The two profiles are however asymmetric, and in the Si III line especially the redshifted peak cannot be fit by a single Gaussian. The profile is rather compatible with a double-peaked emission

Table 1. Emission line measurements. Note that the integrated fluxes are not corrected for reddening and the quoted errors are the 1σ statistical errors.

Ion	Date	Integrated flux (10^{-13} erg s^{-1} cm^{-2})	$V_{\rm blue}$ (km s^{-1})	$V_{\rm red}$ (km s^{-1})	Profile
C III (977 Å)	2001/04/27	7.30 ± 0.11	–650	+670	P-Cyg III
C III (977 Å)	2001/04/29	7.80 ± 0.11	–650	+670	P-Cyg III
C III (1176 Å)	2000/07/22	5.03 ± 0.07	–595	+545	Double peak
C III (1176 Å)	2001/04/27	4.69 ± 0.08	–595	+545	Double peak
C III (1176 Å)	2001/04/29	4.37 ± 0.08	–595	+545	Double peak
Si III (1206 Å)	2000/07/22	22.30 ± 0.08	–740	+870	Double peak
H I Ly α (1215 Å)	2000/07/22	62.00 ± 0.13	–970	+1700	P-Cyg III
N V (1238 Å)	2000/07/22	2.38 ± 0.02	–680	?	Blend with Mg II
O VI (1032 Å)	2001/04/27	6.13 ± 0.06	–560	+600	Double peak
O VI (1032 Å)	2001/04/29	5.84 ± 0.06	–590	+620	Double peak
S VI (933 Å)	2001/04/27	0.44 ± 0.03	–440	+425	Gaussian
S VI (933 Å)	2001/04/29	0.39 ± 0.03	–440	+425	Gaussian

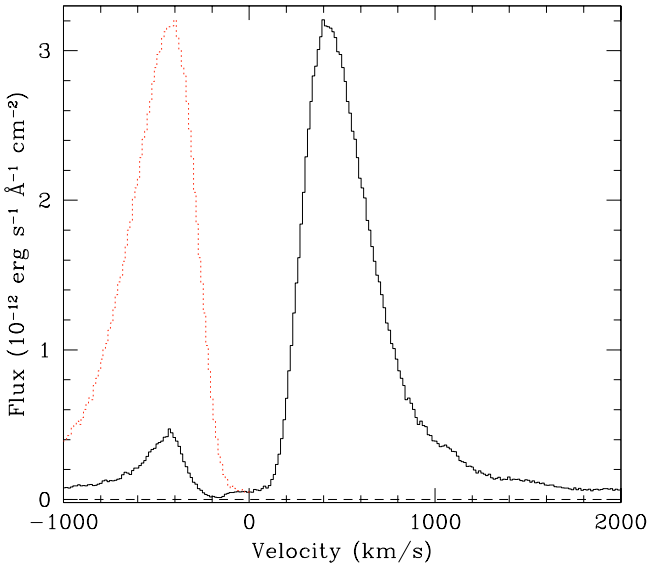

Fig. 2. The H I Ly α line in the STIS spectrum. The dotted line is the reflected profile which provides an estimate of the interstellar contamination to the emission line.

with an additional redshifted peak. This suggests that the line could be formed in two different media.

The H I Ly α line is very broad with wings extending from –970 km s^{-1} to more than 1700 km s^{-1}. The profile is a type III P Cygni, according to Beals (1951), with a strong red emission component and a secondary blueshifted emission peak separated by a deep and broad absorption feature (Fig. 2). At the time of the STIS observation no other absorption component was visible in the profile. We note that part of this broad absorption feature is due to interstellar gas along the line of sight which blurs the exact profile. According to the analysis of the local interstellar medium structure (Lallement & Bertin 1992), the predicted velocity of the local interstellar medium in the direction of the star is about –25 km s^{-1}. This value is in agreement with the radial velocity of the reddest line of the N I triplet lines at 1134.98 Å which is observed in absorption in the *FUSE* spectra. A rough estimate of the contribution of the interstellar gas to the H I Ly α profile can be obtained by reflecting the red wing of the profile about the zero velocity. As may be seen in Fig. 2, the interstellar absorption cannot be responsible for the whole absorption feature. The bluest part of the profile is thus evidence for the presence of wind. We measured a wind terminal velocity of 270 ± 15 km s^{-1} in this blueshifted feature. In spite of the high variability of the hydrogen emission lines, this result is consistent with the analysis of Hα and Hβ Balmer lines made by Pogodin (1994). The author indeed reported night-to-night variations with a main absorption feature slightly blueshifted with a velocity between −50 to –80 km s^{-1}, and a secondary one, blueshifted by about 200 km s^{-1}.

We suspect the presence of the H I Ly β in the *FUSE* spectrum, as a weak and broad emission in the wings of the strong airglow emission. However, the geocoronal emission hides the stellar emission and prevents an analysis of the stellar line profile.

To investigate the behaviour of each line, we measured the radial velocity of the emission line wings and the total line flux of the various lines (Table 1). For the *FUSE* observations, we derived the emission line parameters from the co-addition of the two segments of the same channel in order to increase the signal-to-noise ratios. During the short time-lag between the two *FUSE* observations, no clear variation of these FUV lines occurs, either in shape or in strength, within the instrumental flux accuracy. Indeed, the observed variations in the lines flux exceed the statistical error bars (Table 1); however, the absolute values of the flux given by *FUSE* are subject to uncertainties due to, for instance, channels misalignment and drift of the target within the spectrograph slits. As found from calculating the integrated flux in each individual sub-exposure, this uncertainty is about 15% and prevents us from concluding about the variation of the intensity of the emission lines on a time scale of 2 days.

However, the comparison of the *FUSE* and STIS spectra of the C III* multiplet shows significant changes in line

Table 2. Fe II fluorescent lines in the *FUSE* spectrum of HD 163296. The lines labeled with ([a]) are the transitions identified in HD 104237 by Harper et al. (2001).

λ_{obs}	λ_{vac}	Lower level		Upper level		Comment
(Å)	(Å)	Configuration	Term	Configuration	Term	
	1109.716	$3d^6(^5D)4s$	a $^4D_{5/2}$	$3d^5(^4D)4s4p(^3P^0)$	$^4D_{5/2}$	Blend with λ1109.941
	1109.719	$3d^6(^5D)4s$	a $^6D_{5/2}$	$3d^6(^5D)5p$	$^4F_{7/2}$	Blend with λ1109.941
1109.970	1109.941	$3d^6(^5D)4s$	a $^6D_{7/2}$	$3d^6(^5D)5p$	$^6F_{5/2}$	
	1110.005	$3d^6(^5D)4s$	a $^4D_{3/2}$	$3d^5(^4D)4s4p(^3P^0)$	$^4D_{3/2}$	Blend with λ1109.941
1112.258	1112.151[a]	$3d^6(^5D)4s$	a $^6D_{7/2}$	$3d^6(^5D)5p$	$^6F_{7/2}$	
1113.746	1113.764	$3d^6(^5D)4s$	a $^6D_{3/2}$	$3d^6(^5D)5p$	$^6F_{1/2}$	
	1118.012	$3d^7$	a $^4F_{5/2}$	$3d^5(^4G)4s4p(^3P^0)$	$v^4F_{7/2}$	Blend with λ1118.839
1118.994	1118.839	$3d^7$	a $^4F_{5/2}$	$3d^6(^3F^1)4p$	$u^2D_{3/2}$	
1123.070	1122.843	$3d^6(^5D)4s$	a $^6D_{7/2}$	$3d^5(^4P)4s4p(^3P^0)$	$^6P_{5/2}$	
1127.253	1127.098	$3d^6(^5D)4s$	a $^6D_{9/2}$	$3d^6(^5D)5p$	$^6D_{9/2}$	
1128.274	1128.153	$3d^7$	a $^4F_{7/2}$	$3d^6(^5D)5p$	$^4F_{5/2}$	
	1130.863[a]	$3d^7$	a $^4F_{9/2}$	$3d^6(^5D)5p$	$^6F_{7/2}$	Blend with λ1131.594
1131.677	1131.594[a]	$3d^7$	a $^4F_{5/2}$	$3d^6(^5D)5p$	$^4F_{3/2}$	Blend with λ1130.863 and λ1131.855
	1131.855[a]	$3d^7$	a $^4F_{7/2}$	$3d^6(^5D)5p$	$^4F_{7/2}$	Blend with λ1131.594
1135.254	1135.184	$3d^7$	a $^4F_{3/2}$	$3d^6(^5D)5p$	$^4F_{3/2}$	Blend IS N I and Fe II below
1135.686	1135.302[a]	$3d^7$	a $^4F_{3/2}$	$3d^6(^5D)5p$	$^4D_{1/2}$	
	1135.548[a]	$3d^7$	a $^4F_{5/2}$	$3d^6(^5D)5p$	$^4P_{5/2}$	Blend with λ1135.302
	1135.577[a]	$3d^7$	a $^4F_{5/2}$	$3d^6(^3P^1)4p$	$^4P_{3/2}$	Blend of λ1135.548
1137.401	1137.258[a]	$3d^7$	a $^4F_{3/2}$	$3d^6(^5D)5p$	$^4D_{3/2}$	
1138.989	1138.941[a]	$3d^7$	a $^4F_{5/2}$	$3d^6(^5D)5p$	$^4D_{5/2}$	
1145.683	1145.512	$3d^7$	a $^4F_{7/2}$	$3d^6(^3F^2)4p$	$^4G_{5/2}$	

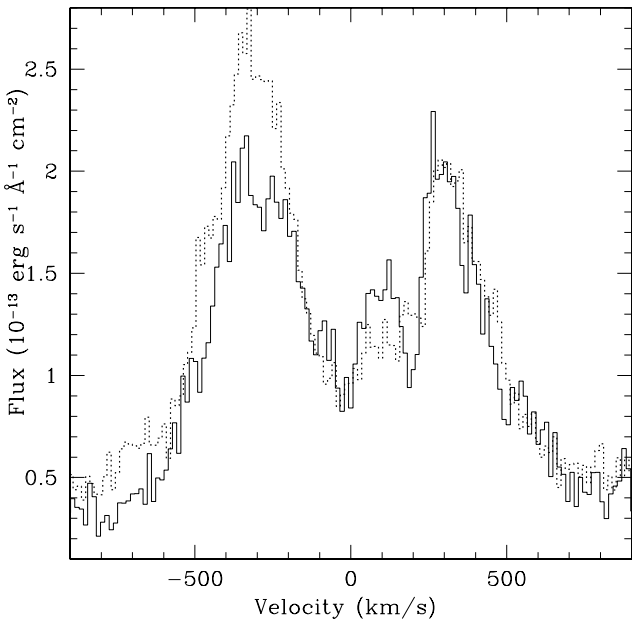

Fig. 3. Temporal variation of the C III* emission line profile: the *FUSE* spectrum rebinned by 8 pixels (2001/04/27, solid line) and the STIS spectrum (2000/07/22, dotted line).

profile: although the wings of the line remain identical and the global profile is double-peaked, the intensity of the blue peak changes (Fig. 3). In addition, a weak, slightly redshifted emission is clearly present in the 2001/04/27 *FUSE* observation indicating that at least part of this ion emission originates from the same region as the C III resonance line. Also, the similarities between the C III* and Si III line profiles show evidence of a common region of formation for these two ions.

These strong and broad emission lines, with various profiles, probe layers above the photosphere with temperatures up to 350 000 K for O VI. All of the line profiles are asymmetric but appear less complex for increasing temperature. The type III P Cygni profile of the H I Ly α line and, most likely, of the C III resonance line, are consistent with an outflow signature.

3.2. Fe II fluorescence emission lines

Conspicuous sharp emission features are observed in the *FUSE* spectra which correspond to transitions from high Fe II levels. Such phenomena have already been reported for HD 104237, another Herbig Ae star (Harper et al. 2001) and in fact the *FUSE* spectra of both stars are very similar in this spectral range. It is difficult to disentangle the emission and the absorption spectra in this spectral region where numerous absorption lines from the stellar photosphere or from the CS/IS gas occur, as seen in Fig. 4. The process of identification in our spectra was thus aided by comparison with the HD 104237 *FUSE* spectrum, in which fluorescent lines of Fe II were identified by Harper et al. (2001), who used an approximate line formation model. The wavelengths of the emission features with the proposed identifications are given in Table 2. Most of these lines

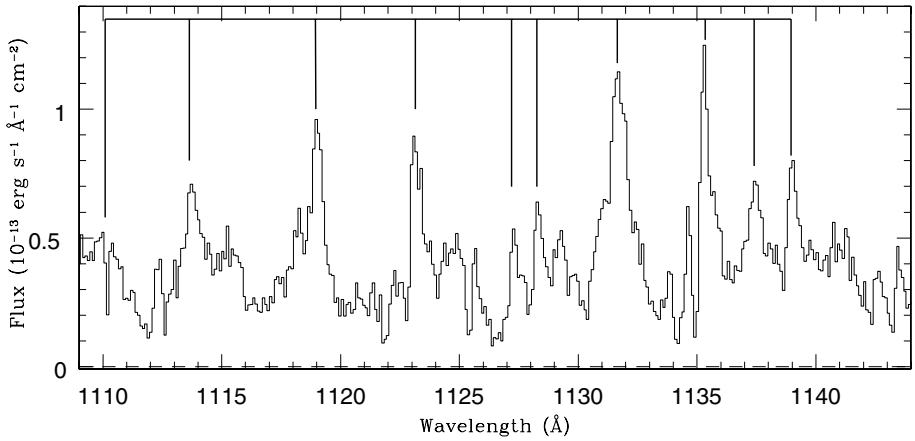

Fig. 4. LiF2a *FUSE* spectrum of HD 163296 recorded on 2001/04/27. The main emission features identified as Fe II fluorescent decays following excitation by H I Ly α are labeled at the top.

correspond to Fe II transitions from the terms ^{4}D°, ^{4}F° and ^{6}D° of the odd configuration 3d^6(^{5}D)5p. A few transitions occurring from upper levels which lie very close in energy as the 3d^6(^{3}F)4p ^{4}G° term are also identified, as well as some from terms of the 3d^5(^{5}D)4s4p(^{3}P^0) configuration which is close to 100 000 cm^{-1}. All the identified lines correspond to decays to the a ^{6}D term of the ground level or the sub levels of the first excited level: 3d^7 a ^{4}F with energy ranging from 1872.56 to 3117.46 cm^{-1}. According to Johansson & Jordan (1984), these upper levels can be populated from the 3d^6(^{5}D)4s a^{4}D levels by photons with wavelength within ±3 Å of the rest wavelength of H I Ly α. As seen in Fig. 2, the H I Ly α wings extend from –3.9 to 6.9 Å and thus the flux available in the line must be sufficient to photo-excite levels around 10 eV in this star.

We observe that the average of the centroids for all the measured lines is redshifted by about 30 km s^{-1} with respect to the stellar velocity. Although the blending of the lines as well as the uncertainty in the exact position of the photospheric flux prevent us from deriving accurate line widths, we measured line widths from 70 km s^{-1} up to more than 170 km s^{-1}. This suggests that the Fe II comes from a spatially extended medium where turbulence or inhomogeneities may be responsible for these widths.

Fluorescent excitation in O I leading to emission lines in the near IR and in the UV resonance triplet at 1304 Å have been reported for the star (Felenbok et al. 1988). The authors suggested pumping by H I Ly β of the ground level to excited upper levels as a likely excitation mechanism for this ion. As described in Sect. 3.1, the H I Ly β appears present in emission. Although the exact shape of the line could not be derived, we measured broad wings extending from –620 km s^{-1} up to roughly +380 km s^{-1}, that is enough to allow the O I excitation to take place. It confirms that the H I Ly β line is the likely pumping mechanism of O I.

4. Discussion

Considering the spectral signatures observed in the HD 163296 spectrum, it is clear that the star presents a number of similarities with AB Aur. The latter is considered as the prototype of a subset of Herbig Ae stars called the P Cygni subclass (Catala et al. 1986) and has been the subject of a number of detailed analyses that give a good understanding of its close environment. HD 163296 shares with AB Aur several spectral characteristics which are interesting to consider in the analysis:

- the H I Balmer lines exhibit considerable profile variability on time scales from one hour to a few days (Pogodin 1994; Beskrovnaya et al. 1998; Catala et al. 1998);
- the profile of the Mg II k and h lines are also highly variable. In HD 163296, the shape of the profile can change from a type III P Cygni to a type IV P Cygni, while this dramatic change has not been observed in AB Aur (Catala et al. 1989, 1986);
- in the visible, the Ca II K resonance line is in absorption and asymmetric. Moreover, the line is blueshifted relative to the star's rest frame with both blue and red edges of the line which vary in time;
- in both stars, a periodic modulation of the Mg II and Ca II line profiles has been found (Catala et al. 1989; Praderie et al. 1986);
- in AB Aur, the He I 5876 Å line profile is made of two distinct components which present different temporal behaviour: the blue component is modulated in velocity with a 45 h period while the red one varies mainly in intensity, changing from an emission to an absorption feature (Catala et al. 1999). In HD 163296 the line profile, as seen on a spectrum available in the Elodie archive at Observatoire de Haute-Provence (OHP), is similar to the resulting profile observed in AB Aur when the redshifted component is in absorption. However, we lack clear information on the temporal behaviour of the line in HD 163296;
- among over-ionized species, the C IV and Si III resonance doublets are the only lines observed in absorption with no emission feature on the red side of the lines. In both stars, the absorption feature is blueshifted. From *IUE* archive spectra of HD 163296 we measured the position of the C IV centroid at about –60 km s^{-1} in the star's rest frame.

This set of common characteristics strongly argues in favour of a similar structure of the close environment around each of

these stars. Indeed, the P Cygni profile observed in Mg II and in the hydrogen lines is strong evidence of a wind while the observations of emission features in various lines are clues for the existence of additional heated layers. For AB Aur, the presence of a wind with an extended chromosphere and a cooler outer region has been established from the comparison of the observed line profiles with a semi-empirical model (Bouret & Catala 1998, and references therein). As demonstrated by these authors, the presence of the C IV resonance doublet lines in absorption implies that the temperature in these regions should be lower than 25 000 K. The Fe II fluorescent features detected in our *FUSE* spectra, complementing the O I lines previously observed in the visible, provide an additional clue for these chromospheric layers as these emission lines should originate in a moderate temperature region. Indeed, according to McMurry et al. (1999), in cool stars these lines are related to a stellar chromosphere where the gas is heated by shocks. In their first analysis of the AB Aur *FUSE* spectrum, Roberge et al. (2001) reported the presence of several unidentified emission lines. We verified that, as in HD 163296, these lines are due to Fe II fluorescent decays, reinforcing the similarities between the close environment of the two stars. The observations of these lines in a group of three Herbig Ae stars, with effective temperatures ranging from about 8500 K for HD 104237 to 9800 K for AB Aur, suggests that the same mechanism able to sustain such a spectral activity is operating in this class of stars.

However, as in the case of AB Aur, such a model cannot account for all of the spectral characteristics, especially for the line profile of over-ionized species like O VI or N V (Bouret et al. 1997). The presence of such emission lines arising in transitions of highly ionized species indicates the presence of hot circumstellar matter, up to 3.5×10^5 K, located close to the stellar surface. The large width of the lines and their asymmetry appear consistent with the presence of more than a single component. The variety of profile types also argues in favour of a composite origin. Another mechanism is thus required to explain at least part of the observed emission.

We thus propose and discuss in the following two plausible mechanisms able to generate the high temperature regions required to explain these new observed emissions.

The first mechanism is magnetic accretion onto the star which involves a circumstellar disk interacting with a magnetically active star. This model is frequently invoked to explain the main CTTS's observational characteristics: strong and broad emission lines, often with time-dependent variations, and an excess emission in the continuum (see Bouvier 2003). With a dipole-like configuration of the stellar magnetic field, the matter from the disk is channeled along the lines of force and reaches the stellar surface at supersonic velocity near the circumpolar regions. The impact of the accreting material onto the stellar surface produces a strong shock, which can appear as a hot spot or a ring, depending the magnetic field configuration. As a result, the gas is heated in the pre- and post-shock regions to temperature of a few 10^6 K (Lamzin 1998). Overionized species are created in these regions, close to the star and a strong continuum excess is also produced. Theoretical studies predict that the resonance lines of C IV, N V and O VI form in the pre-shock and post-shock regions (Lamzin 1998). The resulting line profiles display two emission peaks: one with its centroid velocity close to the stellar one and a second one at a velocity close to the free-fall velocity (Lamzin 2003a,b). The integrated profiles are thus asymmetric, redshifted, with a total width not exceeding the free-fall velocity, which for CTTSs is typically less than 400 km s^{-1}.

For Herbig Ae stars, this mechanism is however not so well established due to the lack of clear observational constraints and specific theoretical developments. In particular, two points deserve more investigations: the observed width of the emission lines and the continuum excess expected from the impact of circumstellar material onto the star which veils the stellar spectrum. For HD 163296 using $R_\star = 2.2\ R_\odot$ and $M_\star = 2.3\ M_\odot$ (Bouwman et al. 2000), the free-fall velocity is about 630 km s^{-1}, a value well below the total width of the observed emission lines, which is typically greater than 1000 km s^{-1} (Table 1). Note, in this context, that even in CTTSs the situation is similar for the well-studied Balmer lines (Muzerolle et al. 1998): the observed large width of the profiles is then explained by the presence of an additional mass outflow driven by open field lines, close to the corotation radius (Beristain et al. 2001).

Concerning the veiling phenomenon in Herbig Ae stars, we lack the necessary observational support as no systematic study has been carried out. AB Aur is the only star for which detailed investigations in the visible show an absence of a noticeable veiling effect (Böhm & Catala 1993). However, this non detection does not definitely rule out the magnetospheric accretion scenario for Herbig Ae stars. Indeed, on the one hand, the veiling effect is more difficult to highlight in stars hotter than the T Tauri stars as, due to the temperature inferred, it should be indistinguishable from the stellar photosphere. On the other hand, the configuration of the accreting column relative to the observer and the physical conditions of the gas could also make the detection difficult. Clearly, this point needs to be further investigated for this class of stars.

An appealing alternative process is the wind confined model proposed by Babel & Montmerle (1997) to explain X-ray emission from Ap and Bp stars. The advantages of this model are that it does not require a disk massive enough to accrete but a mass outflow from the stellar surface, together with, as in the previous scenario, a large scale intense magnetic field. Following the model developed by Babel & Montmerle (1997), the wind from the polar regions is confined and structured in the closed magnetosphere. The two stellar-wind streams from both magnetic hemispheres collide in the magnetic equatorial plane, producing a strong shock. As a result, a large and extended post-shock region where the gas is heated to temperatures up to a few million of Kelvin is created. In addition, the cooling of the material leads to the formation of an ionized disk plasma at the magnetic equator, in corotation with the star in the inner region. In such a scenario, the X-ray emission, but also the over-ionized species, should originate in the post-shock region or in the so-called equatorial disk. Turbulence in regions extending over a few stellar radii with also a large gradient in temperature may participate in the broadening of the line but rotation is the dominant process. In such a scenario, the variations in the mass-loss should naturally act on the post-shock region and

consequently on the intensity of the emission lines. Note that such a model does not require a radiatively-driven wind.

In such a framework, we can provide a rough estimate of the magnetic field intensity. Assuming a dipolar magnetic field, the Alfvén radius, r_A is the distance, in stellar radius, where the kinetic energy balances the magnetic pressure of the dipole:

$$\frac{1}{2}\rho_{r_A} V_{r_A}^2 = \frac{B_{r_A}^2}{8\pi}$$

where ρ_{r_A} is the density, V_{r_A} the velocity of the gas and B_{r_A} the intensity of the magnetic field at the Alfvén radius. Inside this region, the wind is thus frozen into the magnetic field lines connected to the star, and forced to rotate with the angular velocity of the star. Assuming that the type III P Cygni profile of C III is dominated by rotation in the region inside the Alfvén radius, we estimate a rotation velocity of 650 km s^{-1} at the Alfvén radius, measured as the maximum velocity reached in the line wings. Note that this value is consistent with the mean value of about 550 km s^{-1} that can be derived for the Hα type III P Cygni profile, according to Pogodin (1994) and Beskrovnaya et al. (1998). With a $v \sin i$ = 120 km s^{-1} (Halbedel 1996) and assuming that the line broadening is dominated by the rotation of the magnetosphere, we find an Alfvén radius of 5.4 $R_\star$. Under the straightforward assumption of a dipolar configuration, the field behaves as $B = B_\star(R_\star/R)^3$ and is, at the stellar surface:

$$B_\star = \sqrt{\frac{\dot{M} r_A^4 V_\infty}{R_\star^6}}$$

where $\dot{M}$ is the stellar mass loss, V_∞ the terminal velocity. Note that this result is valid under the assumption of a homogeneous and spherically symmetric wind, which is not entirely correct. For the terminal velocity, we took a mean value of 300^{+40}_{-20} km s^{-1} according to the temporal series analysis of the Mg II resonance lines done by Catala et al. (1989). The stellar mass loss was estimated from a set of *IUE* spectra recorded in 1987. We selected and averaged spectra in which the Mg II k line has a clear type III P Cygni profile. The resulting mean observed profile was then modeled with the ETLA code (see e.g. Bouret & Catala 1998) and we derived $\dot{M} = 7.3\times10^{-9}\ M_\odot$ yr^{-1} (Fig. 5). These values give $B_\star \approx 700$ G at the stellar surface. This value is an upper limit to the true potential field, as the magnetic field may exhibit a more complex topology at the stellar surface. Moreover, the rotational modulation of the Mg II and Ca II resonance lines tends to favour a configuration with a magnetic axis tilted with respect to the star's rotational axis.

The presence of a stellar magnetic field in Herbig Ae stars is controversial on both theoretical and observational point of views. Indeed, as these stars lie on radiative tracks, they are not expected to possess outer convective zones which is necessary to sustain a solar-like dynamo. However, alternative sources of magnetic field generation are possible and have been considered by different authors. For instance, the dynamo effect may result from a shear mechanism due to differential rotation which generates a magnetic field (Tout & Pringle 1995; Lignieres et al. 1996). In that case, the efficiency of the generating process is expected to decrease in time leading to the decay of activity signatures and X-ray emission in the corresponding main sequence stars. Another possibility is that some Herbig Ae stars are the progenitors of the Ap-type stars and therefore possess a fossil magnetic field, essentially dipolar. On the observational side, HD 104237 is the only Herbig Ae star for which a detection of magnetic field has been reported (Donati et al. 1997). However, with magnetic field intensity less than 1 kGauss associated with such highly rotating stars, the non-detection by previous surveys does not rule out this possibility and today this issue remains open. Clearly, a higher sensitivity is mandatory and in that field, new instruments such as ESPaDOnS (Manset & Donati 2003), the new generation of spectropolarimeter for CFHT, will provide new insights on this critical point. It is worth mentioning that a value such as the one we derived for the intensity of the magnetic field in HD 163296, is well within the expected performances of ESPaDOnS.

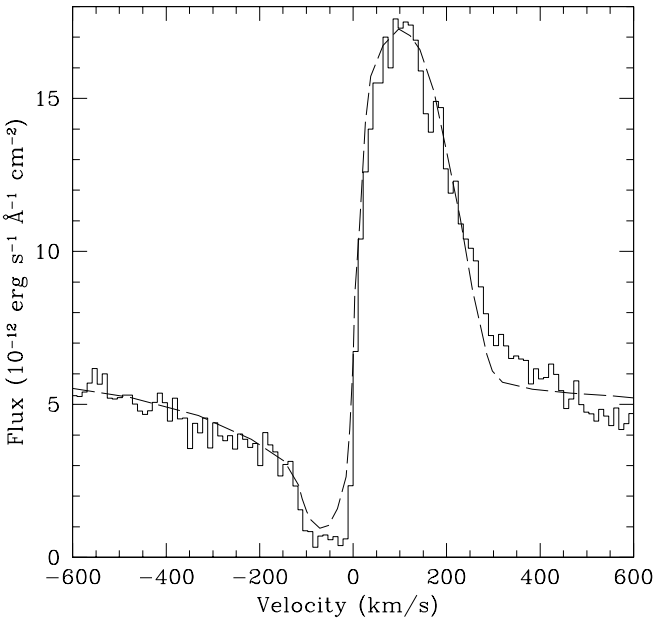

Fig. 5. Observed profile of the Mg II k line (full line) from the *IUE* archives and a synthetic profile (dashed line) computed with ETLA, using $\dot{M}$ = 7.3 $M_\odot$ yr^{-1}.

The magnetically confined wind hypothesis offers the appealing possibility to build a consistent picture of the close stellar environment. It provides a natural explanation for the presence of highly ionized species, the rotational modulation observed in some spectral lines, as well as the X-ray emission recently detected for HD 163296 (Catala et al., in preparation). Indeed, the variability of spectral lines may simply result from the rotational modulation of a magnetosphere when the magnetic axis is tilted with respect to the stellar rotation axis.

A better description of the structure of these hot regions above the photosphere requires a complete modeling of the lines which we intend to present in a forthcoming paper. Also a new set of observations in the FUV range would allow investigations of the temporal behaviour of the different lines and subsequently a better constraint on their formation processes.

Acknowledgements. We thank J. Linsky for his careful reading of an earlier version of the manuscript and his valuable comments and suggestions. This work is based on data obtained for the Guaranteed Time Team by the NASA-CNES-CSA *FUSE* mission operated by the Johns Hopkins University. Financial support to US participants has been provided by NASA contract NAS5-32985. J. C. Bouret is pleased to acknowledge the CNES for financial support.

References

Baade, D., & Stahl, O. 1989, A&A, 209, 268
Babel, J., & Montmerle, T. 1997, ApJ, 485, L29
Beals, C. S. 1951, MNRAS, 111, 202
Beristain, G., Edwards, S., & Kwan, J. 2001, ApJ, 551, 1037
Beskrovnaya, N. G., Pogodin, M. A., Yudin, R. V., et al. 1998, A&AS, 127, 243
Böhm, T., & Catala, C. 1993, A&AS, 101, 629
Bouret, J.-C., & Catala, C. 1998, A&A, 340, 163
Bouret, J.-C., Catala, C., & Simon, T. 1997, A&A, 328, 606
Bouvier, J. 2003, Magnetism and Activity of the Sun and Stars, Proceedings of the conference held 17−21 September, 2002 in Toulouse, France, ed. J. Arnaud, & N. Meunier, EAS Publ. Ser., 9, 287
Bouwman, J., de Koter, A., van den Ancker, M. E., & Waters, L. B. F. M. 2000, A&A, 360, 213
Catala, C., Czarny, J., Felenbok, P., & Praderie, F. 1986, A&A, 154, 103
Catala, C., Donati, J.-F., Böhm, T., et al. 1998, in Cyclical Variability in Stellar Winds, 361
Catala, C., Donati, J. F., Böhm, T., et al. 1999, A&A, 345, 884
Catala, C., Simon, T., Praderie, F., et al. 1989, A&A, 221, 273
Deleuil, M., Lecavelier des Etangs, A., Bouret, J.-C., et al. 2004, A&A, 418, 577
Devine, D., Grady, C. A., Kimble, R. A., et al. 2000, ApJ, 542, L115
Donati, J.-F., Semel, M., Carter, B. D., Rees, D. E., & Collier Cameron, A. 1997, MNRAS, 291, 658
Felenbok, P., Czarny, J., Catala, C., & Praderie, F. 1988, A&A, 201, 247
Finkenzeller, U., & Mundt, R. 1984, A&AS, 55, 109
Grady, C. A., Devine, D., Woodgate, B., et al. 2000, ApJ, 544, 895
Halbedel, E. M. 1996, PASP, 108, 833
Harper, G. M., Wilkinson, E., Brown, A., Jordan, C., & Linsky, J. L. 2001, ApJ, 551, 486
Johansson, S., & Jordan, C. 1984, MNRAS, 210, 239
Lallement, R., & Bertin, P. 1992, A&A, 266, 479
Lamzin, S. A. 1998, Astron. Rep., 42, 322
Lamzin, S. A. 2003a, Astron. Rep., 47, 498
Lamzin, S. A. 2003b, Astron. Rep., 47, 540
Lecavelier des Etangs, A., Deleuil, M., Vidal-Madjar, A., et al. 2003, A&A, 407, 935
Lignieres, F., Catala, C., & Mangeney, A. 1996, A&A, 314, 465
Mannings, V., & Sargent, A. I. 1997, ApJ, 490, 792
Manset, N., & Donati, J. 2003, in Polarimetry in Astronomy, ed. Silvano Fineschi, Proc. SPIE, 4843, 425
McMurry, A. D., Jordan, C., & Carpenter, K. G. 1999, MNRAS, 302, 48
Moos, H. W., Cash, W. C., Cowie, L. L., et al. 2000, ApJ, 538, L1
Muzerolle, J., Calvet, N., & Hartmann, L. 1998, ApJ, 492, 743
Pogodin, M. A. 1994, A&A, 282, 141
Praderie, F., Catala, C., Simon, T., & Boesgaard, A. M. 1986, ApJ, 303, 311
Roberge, A., Lecavelier des Etangs, A., Grady, C. A., et al. 2001, ApJ, 551, L97
Sahnow, D. J., Moos, H. W., Ake, T. B., et al. 2000, ApJ, 538, L7
Sitko, M. L., Grady, C. A., Lynch, D. K., Russell, R. W., & Hanner, M. S. 1999, ApJ, 510, 408
Thé, P. S., Cuypers, H., Tjin A Djie, H. R. E., & Felenbok, P. 1985, A&A, 149, 429
Tout, C. A., & Pringle, J. E. 1995, MNRAS, 272, 528
van den Ancker, M. E., Bouwman, J., Wesselius, P. R., et al. 2000, A&A, 357, 325
van den Ancker, M. E., de Winter, D., & Tjin A Djie, H. R. E. 1998, A&A, 330, 145
Vidal-Madjar, A., Des Etangs, A. L., & Ferlet, R. 1998, Planet. Space Sci., 46, 629